

THE POWER TO SEE



CytoFLEX FLOW
CYTOMETER

Advanced Sensitivity
and Resolution



Mucosal Inducible NO Synthase–Producing IgA⁺ Plasma Cells in *Helicobacter pylori*–Infected Patients

This information is current as of October 28, 2016.

Laura Neumann, Mattea Mueller, Verena Moos, Frank Heller, Thomas F. Meyer, Christoph Loddenkemper, Christian Bojarski, Michael Fehlings, Thomas Doerner, Kristina Allers, Toni Aebischer, Ralf Ignatius and Thomas Schneider

J Immunol 2016; 197:1801-1808; Prepublished online 25 July 2016;
doi: 10.4049/jimmunol.1501330
<http://www.jimmunol.org/content/197/5/1801>

-
- Supplementary Material** <http://www.jimmunol.org/content/suppl/2016/07/23/jimmunol.1501330.DCSupplemental.html>
- References** This article **cites 49 articles**, 19 of which you can access for free at: <http://www.jimmunol.org/content/197/5/1801.full#ref-list-1>
- Subscriptions** Information about subscribing to *The Journal of Immunology* is online at: <http://jimmunol.org/subscriptions>
- Permissions** Submit copyright permission requests at: <http://www.aai.org/ji/copyright.html>
- Author Choice** Freely available online through *The Journal of Immunology* [Author Choice option](#)
- Email Alerts** Receive free email-alerts when new articles cite this article. Sign up at: <http://jimmunol.org/cgi/alerts/etoc>

The Journal of Immunology is published twice each month by
The American Association of Immunologists, Inc.,
9650 Rockville Pike, Bethesda, MD 20814-3994.
Copyright © 2016 by The American Association of
Immunologists, Inc. All rights reserved.
Print ISSN: 0022-1767 Online ISSN: 1550-6606.



Mucosal Inducible NO Synthase–Producing IgA⁺ Plasma Cells in *Helicobacter pylori*–Infected Patients

Laura Neumann,* Mattea Mueller,* Verena Moos,* Frank Heller,[†] Thomas F. Meyer,[‡] Christoph Loddenkemper,[§] Christian Bojarski,* Michael Fehlings,[‡] Thomas Doerner,[¶] Kristina Allers,* Toni Aebischer,^{||,1} Ralf Ignatius,^{#,1} and Thomas Schneider*^{•1}

The mucosal immune system is relevant for homeostasis, immunity, and also pathological conditions in the gastrointestinal tract. Inducible NO synthase (iNOS)–dependent production of NO is one of the factors linked to both antimicrobial immunity and pathological conditions. Upregulation of iNOS has been observed in human *Helicobacter pylori* infection, but the cellular sources of iNOS are ill defined. Key differences in regulation of iNOS expression impair the translation from mouse models to human medicine. To characterize mucosal iNOS-producing leukocytes, biopsy specimens from *H. pylori*–infected patients, controls, and participants of a vaccination trial were analyzed by immunohistochemistry, along with flow cytometric analyses of lymphocytes for iNOS expression and activity. We newly identified mucosal IgA-producing plasma cells (PCs) as one major iNOS⁺ cell population in *H. pylori*–infected patients and confirmed intracellular NO production. Because we did not detect iNOS⁺ PCs in three distinct infectious diseases, this is not a general feature of mucosal PCs under conditions of infection. Furthermore, numbers of mucosal iNOS⁺ PCs were elevated in individuals who had cleared experimental *H. pylori* infection compared with those who had not. Thus, IgA⁺ PCs expressing iNOS are described for the first time, to our knowledge, in humans. iNOS⁺ PCs are induced in the course of human *H. pylori* infection, and their abundance seems to correlate with the clinical course of the infection. *The Journal of Immunology*, 2016, 197: 1801–1808.

Helicobacter *pylori* is a spiral-shaped Gram-negative microaerophilic bacterium that predominantly colonizes the antral region of the human stomach. Although *H. pylori*

infection often remains clinically asymptomatic, a persistent infection-induced inflammation may result in ulceration, atrophy, carcinogenesis, or the development of a MALT B cell lymphoma.

H. pylori acquisition is accompanied by the recruitment of polymorphonuclear and mononuclear cells to the gastric mucosa as well as the generation of specific local and systemic Ab responses (1). Infection also leads to the expression of inducible NO synthase (iNOS or NOS2) as assessed by immunohistochemistry and RT-PCR in gastric mucosal tissue derived from infected patients (2, 3). NO generation by iNOS represents an important antimicrobial effector pathway (4), is a relevant signaling molecule (5, 6), and has been associated with pathological conditions (7). Expression of iNOS has been reported in gastric cancer and MALT lymphoma (8). Although iNOS mRNA or protein has been described in *H. pylori* infection, the cellular source of iNOS—and whether NO is produced—remains unclear. This is mainly due to significant differences between cell types and, importantly, species in the mechanisms controlling gene expression and enzyme activity of iNOS (9). Thus, findings obtained in murine models (10, 11) are difficult to translate to the situation in patients. To date, iNOS expression in the gastric tissue of *H. pylori*–infected patients has been attributed to polymorphonuclear neutrophils and mononuclear cells (2). The present study aimed at further characterizing these iNOS-producing mononuclear cells by means of lineage markers in *H. pylori*–infected individuals, including a cohort of volunteers who had been experimentally infected in the course of a prior clinical *H. pylori* vaccination trial. By applying a combined immunohistochemistry and flow cytometry approach, we identified human IgA⁺ plasma cells (PCs) as a novel major source of NO in *H. pylori*–infected patients as well as in immunized or challenged study participants. Moreover, increased numbers of iNOS⁺ PCs correlated with clearance of experimental infection.

*Medical Clinic I, Gastroenterology, Infectious Diseases and Rheumatology, Charité–University Medicine Berlin, 12203 Berlin, Germany; [†]Practice for Gastroenterology, 12163 Berlin, Germany; [‡]Department of Molecular Biology, Max Planck Institute for Infection Biology, 10117 Berlin, Germany; [§]PathoTres Practice for Pathology, 12247 Berlin, Germany; [¶]Department of Medicine, Rheumatology and Clinical Immunology, Charité–University Medicine Berlin, 10117 Berlin, Germany; ^{||}Robert Koch Institute, 13302 Berlin, Germany; and [#]Institute for Microbiology and Hygiene, Charité–University Medicine Berlin, 12203 Berlin, Germany

¹T.A., R.I., and T.S. contributed equally to this work and are cosenior authors.

ORCID: 0000-0002-7870-7722 (L.N.); 0000-0002-3340-5122 (M.M.); 0000-0001-8695-8081 (C.L.).

Received for publication June 12, 2015. Accepted for publication June 20, 2016.

This work was supported by research funding from the Deutsche Forschungsgemeinschaft (Grants SFB633 and TPB12).

T.A., R.I., and T.S. designed the study; L.N., M.M., V.M., M.F., and C.L. performed experiments; F.H., C.L., T.S., and C.B. collected patient samples; L.N. and M.M. analyzed data and made the figures; L.N., V.M., T.F.M., T.D., K.A., T.A., R.I., and T.S. discussed and interpreted the data; V.M., T.A., and T.S. supervised the research; L.N. and T.A. wrote the manuscript; T.F.M., T.A., R.I., and T.S. obtained funding; F.H., T.D., and T.F.M. provided technical and material support; all authors read and approved the manuscript.

Address correspondence and reprint requests to Prof. Thomas Schneider, Medical Clinic I, Gastroenterology, Infectious Diseases and Rheumatology, Charité–University Medicine Berlin, Hindenburgdamm 30, 12203 Berlin, Germany. E-mail address: thomas.schneider@charite.de

The online version of this article contains supplemental material.

Abbreviations used in this article: B-LCL, B lymphoblastoid cell line; DAF-FM, 4-amino-5-methylamino-2',7'-difluorofluorescein diacetate; hpf, high-power field; iNOS, inducible NO synthase; LPL, lamina propria lymphocyte; mBC, memory B cell; MUM, multiple myeloma oncogene; PC, plasma cell; p.i., postinfection; qPCR, quantitative real-time PCR.

This article is distributed under The American Association of Immunologists, Inc., [Reuse Terms and Conditions for Author Choice articles](#).

Copyright © 2016 by The American Association of Immunologists, Inc. 0022-1767/16/\$30.00

Materials and Methods

Patients, study participants, and collection of specimens

This study and the prior vaccination trial were approved by the Human Research Ethics committee at Charité Berlin (applications EA1/062/11 and 226-05a). Written consent was given by all participants. Gastric antrum biopsy specimens were collected consecutively from 67 patients undergoing upper endoscopy (Table I). Subjects were grouped into *H. pylori*-positive patients and *H. pylori*-negative controls according to the histopathological results obtained by Warthin–Starry silver staining and the rapid urease test on biopsy specimens. In addition, 24 antrum biopsy specimens from participants of a prospective, randomized controlled vaccination study (Paul Ehrlich Institute application 1097/01) conducted in 2006 at the Medical Clinic I, Charité, Campus Benjamin Franklin, Berlin (12), were examined by immunohistochemistry (Table I). These participants, seronegative for *H. pylori* and without evidence of active *H. pylori* infection, had been immunized orally with live attenuated recombinant *Salmonella enterica* serovar Typhi Ty21a strain containing an *H. pylori* urease-expression plasmid (pUreA/B) or a plasmid expressing the *H. pylori* Ag HP0231 (pHP0231). The control volunteers had been treated with Ty21a holding the plasmid pDB2 only. The participants had been challenged with an attenuated *H. pylori* strain [Baylor strain (13)] 42 d postvaccination. Gastric antrum biopsy specimens had been collected 4 wk postvaccination and 6 and 10 wk postchallenge. Active *H. pylori* infection had been diagnosed by the [¹³C] urea breath test, rapid urease test on biopsy specimens, *H. pylori* detection by Warthin–Starry's silver staining of biopsy sections, and culture from biopsy specimens. Although the vaccines tested did not show sufficient protection, in some participants infection was cleared before antibiotic therapy was initiated 10 wk postchallenge. For the purpose of the current study, participants were grouped into 1) those who had eradicated *H. pylori* before the study endpoint ($n = 7$) and 2) those with persistent infection throughout the study period ($n = 17$). Furthermore, duodenal biopsy specimens of untreated patients infected with *Tropheryma whipplei* ($n = 10$), HIV ($n = 10$), or *Giardia duodenalis* (also known as *G. lamblia*) ($n = 10$) were analyzed by immunohistochemistry (Table I).

Immunohistochemistry

Biopsy specimens of 16 *H. pylori*-negative patients, 33 *H. pylori*-positive patients, and 24 study participants as well as biopsy specimens of untreated patients infected with *T. whipplei* ($n = 10$), HIV ($n = 10$), and *G. duodenalis* ($n = 10$) were analyzed by immunohistochemistry. Immunohistological staining on paraffin sections was performed for antral biopsy specimens as described previously (14). Mouse anti-human–multiple myeloma oncogene (MUM)1 (clone MUM1p; Dako, Hamburg, Germany) (15), mouse anti-human-PAX5 (clone 3A7; LifeSpan BioSciences, Eching, Germany), rabbit anti-human-IgA (LifeSpan BioSciences), mouse anti-human-CD68 (Dako), and rabbit anti-human-iNOS (Abcam, Cambridge, U.K.) were used as primary Abs. Stains were visualized using donkey anti-mouse or donkey anti-rabbit biotin (Dianova, Hamburg, Germany), streptavidin–alkaline phosphatase, and Fast red or EnVision (all by Dako). Negative controls were performed by omitting the primary Ab or the biotinylated secondary Ab, respectively. Positive cells were determined as the mean cell counts of 3–10 high-power fields (hpf) of 0.237 mm² each.

Preparation of lamina propria lymphocytes

Biopsy specimens of 13 *H. pylori*-negative controls and 13 *H. pylori*-positive patients were investigated by flow cytometry. Lamina propria lymphocytes (LPLs) were isolated from antral biopsy specimens by collagenase type II (Sigma) digestion (16). Samples were incubated in 10 ml RPMI 1640 (Life Technologies by Life Technologies) containing 7.5% FCS (Sigma), 0.5 mg/ml collagenase type II-S (sterile filtered) (clostridiopeptidase A derived from *Clostridium histolyticum*; Sigma), 0.1 mg/ml trypsin inhibitor (from *Glycine max*; Sigma), and 0.1 mg/ml DNase I (Roche, Berlin, Germany) for 15 min at 37°C and 5% CO₂, with intermittent shaking. Tissue fragments were further disrupted using a 10-cm³ disposable syringe attached to a blunt-ended 16-gauge needle. LPLs were separated from adjacent epithelial cells by Percoll gradient (35%/60%) centrifugation (20–30 min, 2400 rpm) (GE Healthcare, Uppsala, Sweden).

Generation of B-lymphoblastoid cell lines

B-lymphoblastoid cell lines (B-LCL) were established as previously described by transforming B cells from PBMCs with EBV released by the marmoset lymphocyte cell line B95-8 (DSMZ ACC 100; Deutsche Sammlung für Mikroorganismen und Zellkulturen, Braunschweig, Germany) (17). The B cell nature of the cell lines was routinely verified by flow cytometry (FACSCalibur with the Cell Quest Pro software; BD Biosciences, Heidelberg, Germany) upon staining for CD19–allophycocyanin (clone HIB19; BD).

Flow cytometry

To detect surface and intracellular molecules, LPLs were incubated with fluorochrome-labeled Abs, with or without prior fixation with paraformaldehyde (Sigma), and permeabilization with saponin (Sigma), according to previously published protocols (18). The following fluorochrome-labeled anti-human mAbs were used: anti-CD3–allophycocyanin-H7 (clone SK7; BD), anti-CD14–allophycocyanin-H7 (clone M ϕ P9; BD), anti-CD19–PE-Cy7 (clone SJ25C1; BD), anti-CD19–V500 (clone HIB19; BD), anti-CD19–allophycocyanin (clone HIB19; BD), anti-CD20–Pacific Orange (clone HI47; Invitrogen by Life Technologies), anti-CD20–PerCP (clone 2H7; eBioscience, Frankfurt am Main, Germany), anti-CD27–PE (clone O323; eBioscience), anti-CD38–PerCP-Cy5.5 (clone HIT2; BD), anti-CD38–PE-Cy7 (clone HIT2; BD), anti-iNOS–Alexa Fluor 405 (clone C11; Santa Cruz Biotechnologies, Heidelberg, Germany), anti-IgA–allophycocyanin (clone IS11-8E10; Miltenyi Biotec, Bergisch Gladbach, Germany).

A panel of seven colors, including Abs against CD3/CD14, CD19, CD20, CD27, CD38, iNOS, and IgA, was used to characterize PCs by high-dimensional flow cytometry and the gating technique of fluorescence minus one controls.

For the detection of live NO-producing cells, 4-amino-5-methylamino-2',7'-difluorofluorescein diacetate (DAF-FM; Molecular Probes, Eugene, OR) was added to the staining solution (25 μ g/ml) and incubated at room temperature for 30 min (19). The specificity of DAF-FM for NO is very high because diaminofluorescein does not react in neutral solution with mobile and stable oxidized forms of NO, such as NO₂⁻ and NO₃⁻, or other reactive oxygen species, such as O₂⁻, H₂O₂, and ONOO⁻. Under physiological conditions, triazolofluorescein is not formed in the absence of NO (20). After washing with PBS/0.2% BSA, DAPI (Molecular Probes) was added immediately before flow cytometric analysis to exclude dead cells.

For the detection of intracellular cytokines, the cells were incubated for 3 h with 10 μ g/ml Brefeldin A (Sigma). The following fluorochrome-labeled anti-human mAbs were used: anti-IL-1 β -FITC (AS10; BD), anti-IL-2-PE (MQ1-17H12; BD), anti-IL-4-PE (8D4-8; BD), anti-IL-6-FITC (MQ2-6A3; BD), anti-IL-8-FITC (AS14; BD), anti-IL-10–Alexa Fluor 647 (JES3-9D7; eBioscience), anti-TNF- α -PE (MAB11; BD), and anti-IFN- γ -FITC (clone B27; BD).

Cells were analyzed using a FACSCanto II cytometer (BD) running with a DivaSoft operation system (BD). Cell aggregates were excluded according to width versus area of the forward and side scatter signal. Cytometric fluorescence data are displayed as two-dimensional plots using log₁₀ scales, light scatter data on a linear scale.

Quantitative real-time PCR

Isolated LPLs and PBMCs were stained for PC and B cell surface markers. A total of 10²–10⁴ PCs (DAPI⁻CD3⁻CD14⁻CD19⁺CD20⁻CD27⁺CD38⁺) and memory B cells (mBCs) (DAPI⁻CD3⁻CD14⁻CD19⁺CD20⁺CD27⁺CD38⁻) were sorted on a FACSAria II cell sorter (BD Biosciences). RNA was isolated from cells with peqGOLD RNAPure (Peqlab Biotechnologie GmbH, Erlangen, Germany), and cDNA was prepared using the High Capacity cDNA Reverse Transcription Kit (Applied Biosystems by Life Technologies). The expression levels of five genes were determined using TaqMan real-time PCR after TaqMan assay-based preamplification (both Life Technologies). Quantitative real-time PCR (qPCR) amplification was performed using the StepOnePlus Real-Time PCR Systems (Life Technologies). The qPCR included *GAPDH*, as housekeeping gene; *IFN- γ* ; *TNF- α* , and *IL-10* as genes of interest; and *IL-6*, as reference gene for the comparative C_t method.

Statistical analyses

Quantitative parameters are presented as single measurements with medians and interquartile ranges. Data were analyzed using the nonparametric Mann–Whitney *U* test (two-tailed) or the Friedman test with Dunn's post hoc analysis using GraphPad Prism version 5.0. The *p* values < 0.05 were considered significant, as were *p* values < 0.017 when a Bonferroni correction was performed.

Results

PCs constitute one third of mucosal iNOS⁺ cells in *H. pylori*-infected patients

We investigated biopsy specimens from the stomach mucosa by immunohistochemistry to identify the cellular sources of iNOS. Significantly higher numbers of iNOS-expressing cells were found in the mucosa of *H. pylori*-infected patients than in tissue of uninfected controls ($p = 0.0002$, Fig. 1). Macrophages had been

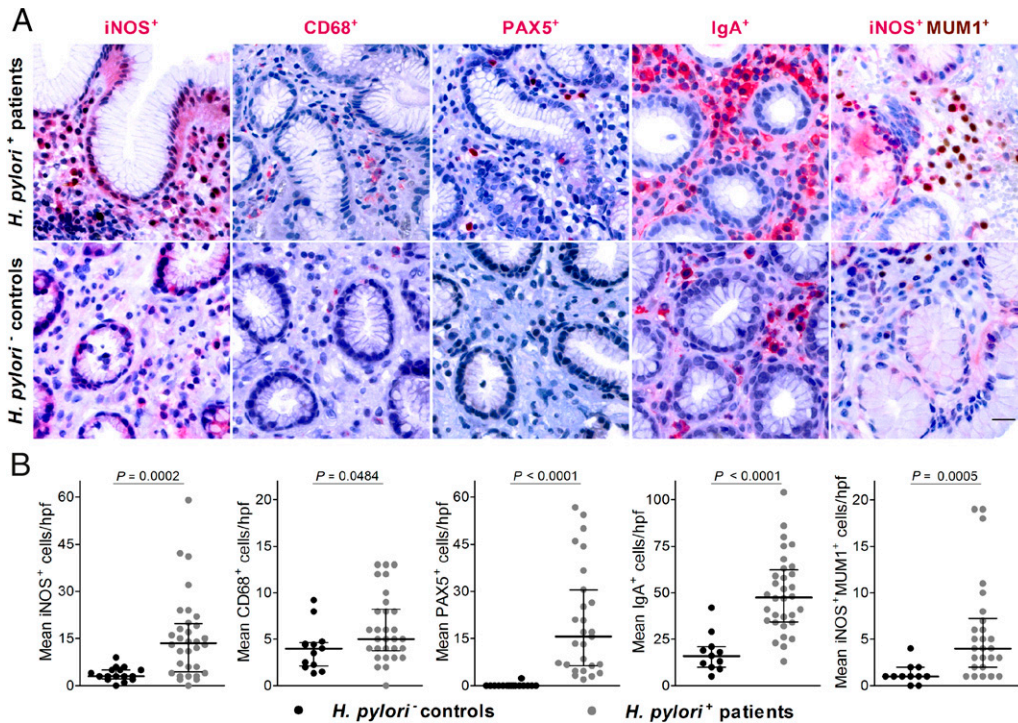


FIGURE 1. The antral mucosa of *H. pylori*-infected patients contains enhanced numbers of iNOS⁺, CD68⁺, PAX5⁺, and IgA⁺ cells as well as iNOS⁺MUM1⁺ PCs. **(A)** Representative immunohistochemically stained paraffin sections of mucosal biopsy specimens of *H. pylori*-negative controls (*H. pylori*⁻) and *H. pylori*-infected patients (*H. pylori*⁺). iNOS-expressing cells were identified by anti-iNOS Ab, macrophages by anti-CD68 Ab, B cells by anti-PAX5 Ab, and PCs by anti-IgA Ab. iNOS-producing PCs were visualized by double staining of anti-MUM1 and anti-iNOS Ab. Scale bar, 20 μm. **(B)** Quantitative analysis of iNOS⁺ cells, CD68⁺ cells, Pax5⁺ cells, IgA⁺ cells, and iNOS⁺MUM1⁺ cells in the antral mucosa of uninfected controls (*n* = 16, black) and *H. pylori*⁺ patients (*n* = 38, gray). Positive cells were counted per hp/hpf and depicted as median plus interquartile ranges (Mann–Whitney test).

implicated as iNOS-expressing cells (2). Expectedly, numbers of CD68⁺ macrophages were increased in patients compared with controls (*p* = 0.0484, Fig. 1); however, the cells constituted only approximately one third of iNOS-expressing cells in the gastric mucosa of patients with *H. pylori* infection (Fig. 1). Morphologically, the appearance of a sizable proportion of iNOS⁺ cells was similar to that of PCs. Thus, we analyzed the histological sections for expression of the B cell lineage-specific markers, Pax5 or BSAP, specific for B cells (21), IgA, and MUM1, which is expressed by PCs and some germinal center B cells (15). Mucosal infiltration of Pax5⁺ B cells and IgA-producing PCs in patients was significantly greater than in controls (*p* < 0.0001, Fig. 1). In addition, we identified MUM1⁺ PCs as a major iNOS-expressing cell type (*p* = 0.0003, Fig. 1) in patients. Approximately one third of the iNOS⁺ cells were MUM1⁺ PCs, whereas this cell type was barely found in biopsy specimens of controls (Fig. 1). To investigate if the presence of iNOS⁺MUM1⁺ PCs is a common feature of response to gastrointestinal infections, we also analyzed mucosal biopsy specimens of untreated

patients with other infectious diseases of the gastrointestinal tract, that is, of untreated patients infected with 1) *Tropheryma whippelii*, a further bacterial infection; 2) HIV; or 3) *Giardia duodenalis* (also known as *G. lamblia*), a parasitic infection associated with IgA-mediated immunity (Table I). None of the samples from patients with these infectious diseases showed iNOS⁺MUM1⁺ PCs in mucosal tissues (Supplemental Fig. 1).

Early increase of mucosal iNOS-expressing PCs following H. pylori infection in previously uninfected individuals

Antral biopsy specimens from participants of an *H. pylori* vaccination trial (12) provided a unique opportunity to examine the kinetics of iNOS⁺ cells within the first few weeks following experimental *H. pylori* infection. The numbers of iNOS⁺ cells, IgA⁺ cells, and iNOS⁺MUM1⁺ PCs were determined using immunohistochemistry on samples collected before infection and 6 and 10 wk postinfection (p.i.). Before *H. pylori* challenge, all volunteers showed similarly low numbers of iNOS⁺ and IgA⁺ cells as well as iNOS⁺MUM1⁺ cells

Table I. Characteristics of patients and study participants

| | Patients | | <i>H. pylori</i> -Positive Study Participants | | | | <i>Giardia duodenalis</i> Patients |
|------------------------|-------------------------------------|-------------------------------------|---|------------|--------------------------------------|--------------|------------------------------------|
| | <i>H. pylori</i> -Positive Patients | <i>H. pylori</i> -Negative Controls | Eradicated ^a | Persistent | <i>Tropheryma whippelii</i> Patients | HIV Patients | |
| No. | 43 | 24 | 7 | 17 | 10 | 10 | 10 |
| Age, median (range) | 56 (20–88) | 52 (29–83) | 29 (27–48) | 30 (24–46) | 57 (42–67) | 51 (34–75) | 48 (38–74) |
| Sex, no. men/no. women | 15/28 | 7/17 | 7/0 | 17/0 | 9/1 | 7/3 | 8/2 |
| Biopsy analysis | | | | | | | |
| Histology | 33 | 16 | 7 | 17 | 10 | 10 | 10 |
| Flow cytometry | 13 | 13 | | | | | |

^aIndependent of the vaccine used.

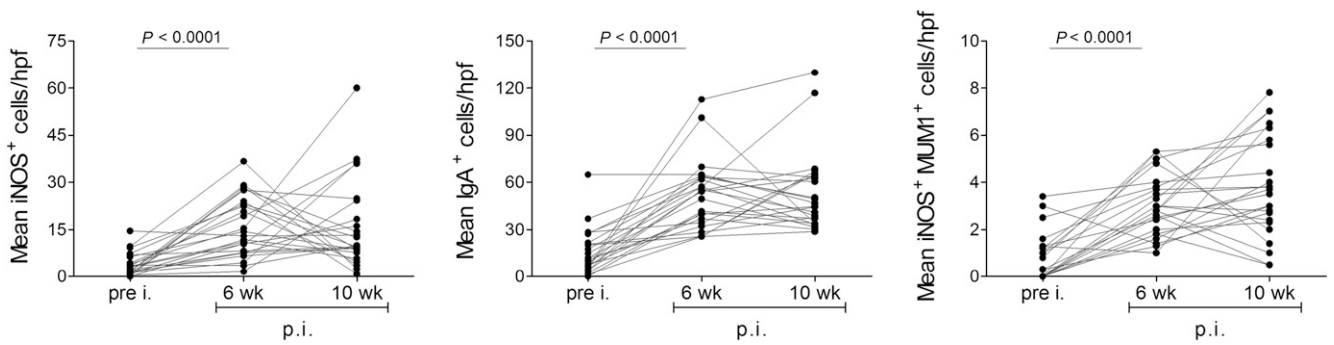


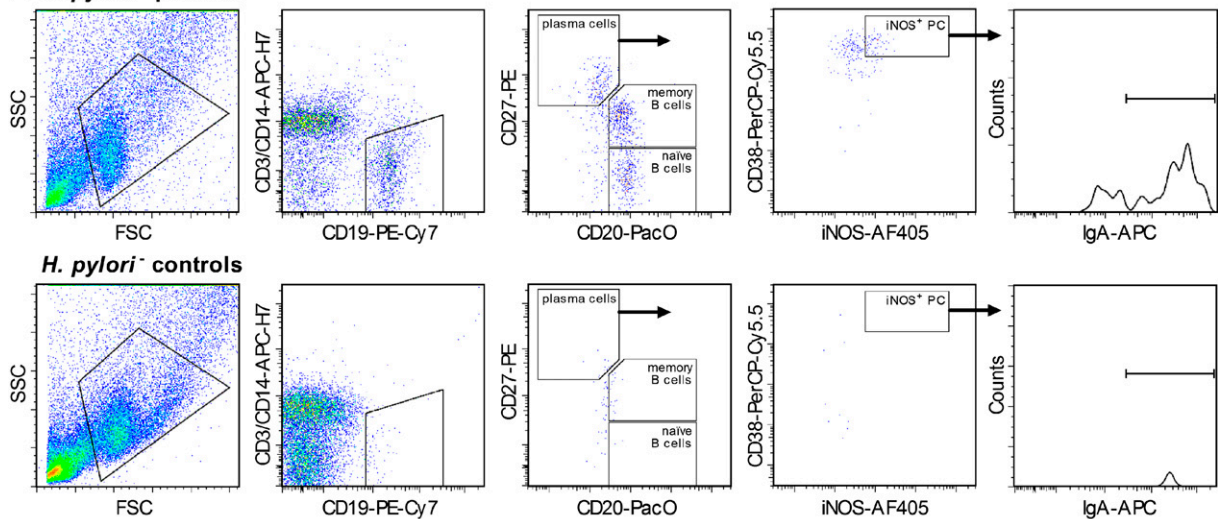
FIGURE 2. Early mucosal influx of iNOS⁺ cells, IgA⁺ cells, and iNOS⁺MUM1⁺ PCs in experimental human *H. pylori* infection. Quantitative analysis of iNOS⁺ cells, IgA⁺ cells, and iNOS⁺MUM1⁺ cells in the antral mucosa of study participants ($n = 24$) at preinfection (pre i.) as well as 6 and 10 wk (wk) p.i. with *H. pylori*. Immunohistochemical staining was performed on paraffin sections. Positive cells per hpf are depicted as associated values over time. Data were analyzed with the Friedman test with Dunn's post hoc analysis.

(Fig. 2). In accordance with data from the prior trial, the vaccination alone had no detectable effect on the gastric mucosa and did not induce significant changes in local cytokine production (12). In contrast, increased numbers of iNOS⁺ cells (14 cells per hpf), IgA⁺ cells (54 cells per hpf), and iNOS⁺MUM1⁺ PCs (3 cells per hpf) were detected in the mucosa at 6 wk p.i. ($p < 0.0001$, Fig. 2). Cell numbers remained increased at 10 wk p.i. (Fig. 2) and were in the same range as in patients chronically infected with *H. pylori* (Fig. 1). Importantly, vaccination did not exacerbate inflammation (12).

High infiltration of CD19⁺ cells, including iNOS-expressing PCs, in the mucosa of H. pylori-infected patients

Because iNOS⁺ PCs had not been described before in humans, we characterized the mucosal PCs in more detail and determined by flow cytometry the percentages of CD19⁺, CD19⁺CD20⁻CD27⁺⁺ (PCs), CD19⁺CD20⁺CD27⁺ (mBCs), and CD19⁺CD20⁺CD27⁻ (naive B cells) in the stomach mucosa of *H. pylori*-infected patients (Fig. 3A). Of isolated LPLs, ~20% were CD19⁺ cells (Fig. 3B). These comprised PCs (10.2% among all CD19⁺) and also memory

A *H. pylori*⁺ patients



B

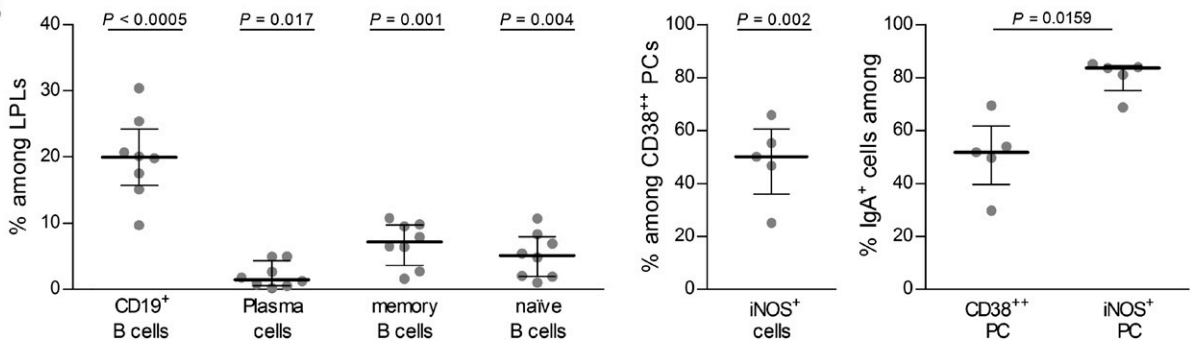
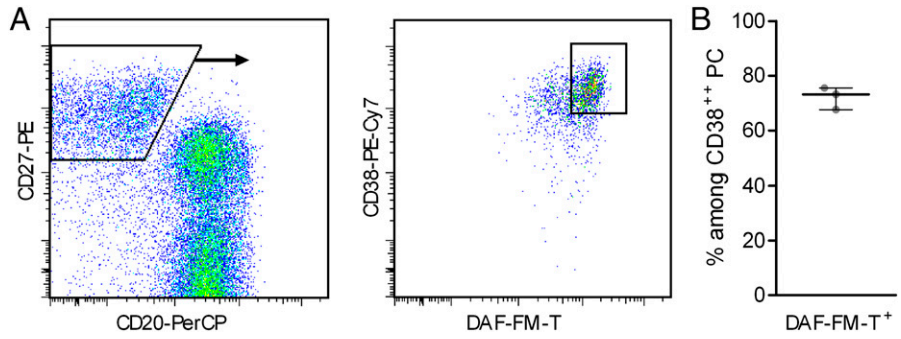


FIGURE 3. Infiltration of B cells and iNOS-expressing PCs in *H. pylori*⁺ patients. **(A)** Representative gating strategy for analysis of LPLs by flow cytometry: 1) gating on lymphocytes by forward (FSC) and side scatter (SSC) properties; 2) exclusion of T cells (CD3⁺) and monocytes (CD14⁺) and gating on CD19⁺ B cells; 3) detection of PCs (CD20⁻CD27⁺⁺), mBCs (CD20⁺CD27⁺), and naive B cells (CD20⁺CD27⁻); 4) detection of iNOS⁺CD38⁺⁺ PCs; and 5) detection of IgA⁺ PCs within iNOS⁺CD38⁺⁺ PCs. **(B)** Quantitative analysis of the flow cytometric data of *H. pylori*-infected patients according to the gating strategy. Values are depicted as median plus interquartile ranges (Mann-Whitney *U* test).

FIGURE 4. Detection of NO-producing PCs in *H. pylori*-infected patients. (A) Representative gating strategy for the analysis of CD19⁺CD3⁻CD14⁻DAPI⁻ PCs of *H. pylori*-infected patients by flow cytometry: gating on PCs (CD20⁻CD27⁺⁺) within all CD19⁺ B cells, and then on CD38⁺⁺DAF-FM-T⁺ PCs. (B) Quantitative analysis of the data of *H. pylori*⁺ patients (*n* = 3). Values are depicted as median plus interquartile ranges.



and naive B cells (38.9 and 22.9% among all CD19⁺, respectively), and were increased in *H. pylori*-infected patients compared with uninfected controls (Fig. 3A). LPLs of control patients contained almost no CD19⁺ B cells, which is in agreement with previous studies (22). We additionally characterized by flow cytometry the PCs (CD19⁺CD20⁻CD27⁺⁺) for the expression of CD38, to distinguish them further from mBCs (CD38⁻), and for iNOS. Notably, 50% of the mucosal CD38⁺⁺ PCs in *H. pylori*-infected patients expressed iNOS and 84% of these expressed IgA (Fig. 3B).

As the presence of iNOS protein does not necessarily reflect active enzyme (9), we investigated the functionality of iNOS enzyme in iNOS⁺ PCs. Intracellular NO production was visualized by flow cytometry using DAF-FM-T (19). Analysis of LPLs isolated from biopsy specimens obtained from infected individuals (Fig. 4) showed consistently that ~70% of all CD19⁺CD27⁺⁺CD38⁺⁺CD20⁻CD3⁻CD14⁻DAPI⁻ PCs became DAF-FM-T⁺ PCs; that is, these PCs expressed enzymatically active iNOS and produced NO (Fig. 4B).

Eradication of H. pylori is accompanied by increased numbers of mucosal iNOS⁺ PCs

In the prior vaccination trial (12), some individuals had cleared the experimental *H. pylori* infection, whereas the majority had not, and this correlated with *H. pylori*-specific T cell responses (12). To investigate whether the course of infection may also be positively or negatively correlated with gastric iNOS⁺ PCs, we quantified the numbers of iNOS⁺ cells, IgA⁺ cells, and iNOS⁺MUM1⁺ PCs in study participants who had eradicated *H. pylori* (*n* = 7) and individuals who had remained infected throughout the study (*n* = 17). Before *H. pylori* challenge, both groups showed similarly low numbers of iNOS⁺ and IgA⁺ cells as well as iNOS⁺MUM1⁺ cells (Fig. 5). Total numbers of iNOS⁺ cells were increased at week 6 p.i. in individuals of both groups. At 10 wk p.i.,

there was a trend toward reduced total numbers of iNOS⁺ cells in both groups (Fig. 5). Numbers of IgA⁺ cells were also significantly increased in both groups at 6 wk p.i. and remained high and at comparable levels in both groups (Fig. 5). In contrast, the number of iNOS⁺MUM1⁺ PCs—although being comparable in both groups at 6 wk p.i. (Fig. 5)—was significantly higher at 10 wk p.i. in those study participants who had eradicated *H. pylori* (Fig. 5).

iNOS-expressing B lineage cells produce pro- and anti-inflammatory cytokines

Finally, we investigated whether the iNOS expression is associated with B cell effector functions such as cytokine production. To ensure sufficient cell numbers for these experiments, we used EBV-transformed B cells as a model to study the expression of CD38 and iNOS, as well as the production of different pro- and anti-inflammatory cytokines, including IL-1β, IL-2, IL-6, IL-8, TNF-α, IFN-γ, IL-4, and IL-10. According to previous studies, EBV transformation of primary human B cells changes various cellular properties (23, 24), such as the expression of the cell activation-associated Ag CD38 (25), and the expression of iNOS (26). Furthermore, B-LCLs have been described as expressing various cytokines with a high degree of heterogeneity (24, 27–32). In our B-LCL, iNOS expression was detectable in highly activated CD38⁺⁺ EBV-infected B cells, but not in CD38⁺ or CD38⁻ B cells (Fig. 6A). In addition, the highly activated B-LCL cells expressed the proinflammatory cytokine IFN-γ (Fig. 6A), but the other cytokines have not been produced in our B-LCL (data not shown). Notably, IFN-γ production was limited to iNOS-expressing B cells (Fig. 6B).

Furthermore, we investigated the cytokine gene expression of B lineage cells during *H. pylori* infection. Sorted PCs and mBCs from isolated LPLs and PBMCs of an *H. pylori*-infected patient were analyzed for relative gene expression of pro- and anti-inflammatory cytokines by qPCR. Mucosal mBCs showed a higher expression level

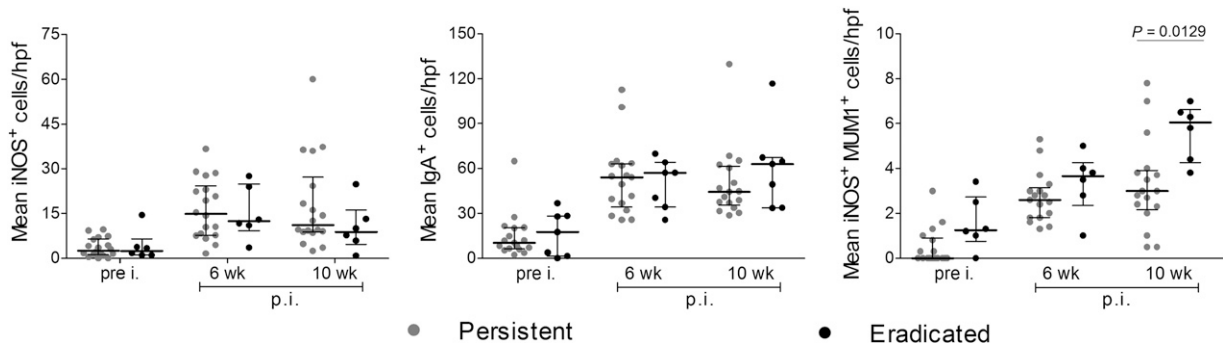
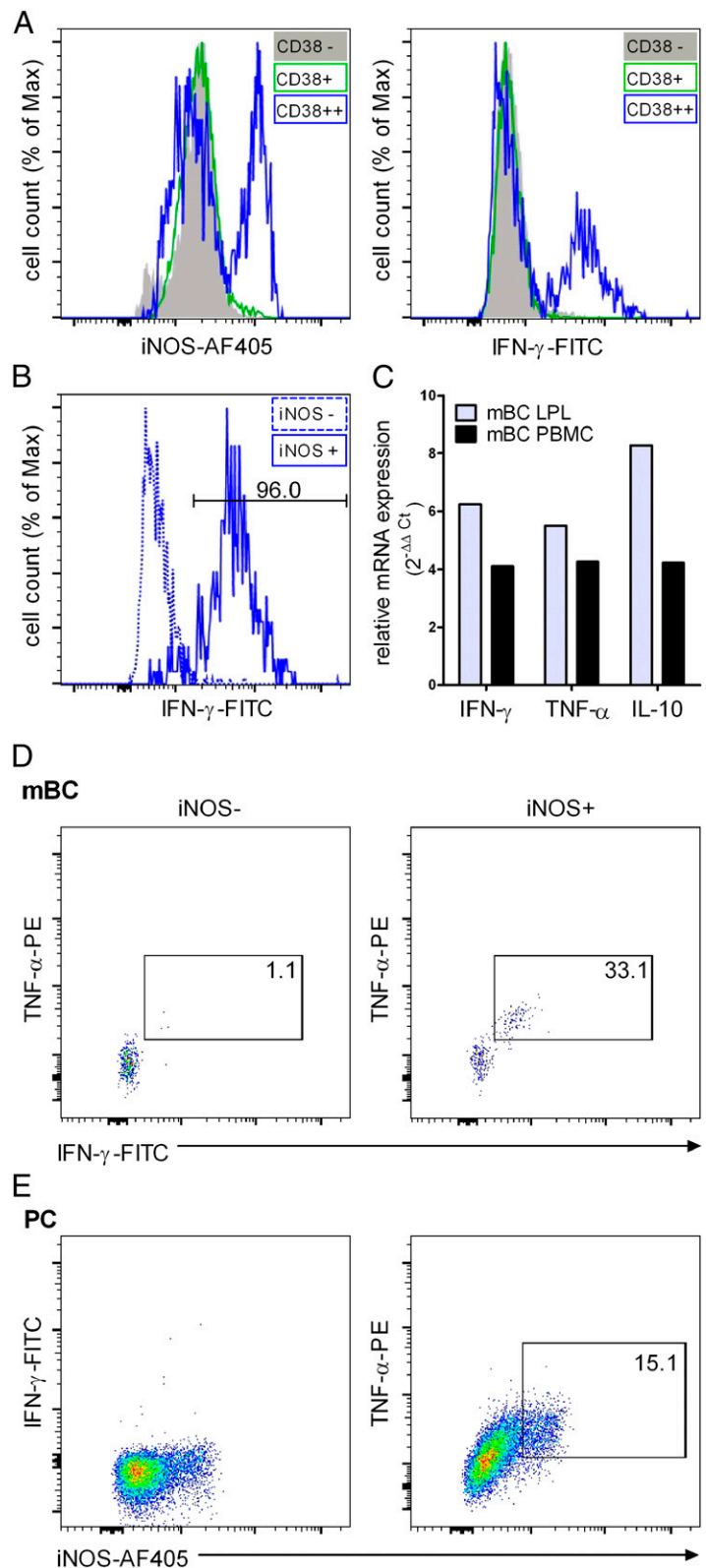


FIGURE 5. Increased numbers of iNOS⁺ PCs in the antral mucosa of individuals able to eradicate *H. pylori*. Quantitative analysis of iNOS⁺ cells, IgA⁺ cells, and iNOS⁺MUM1⁺ cells in the antral mucosa of subjects preinfection (pre i.) as well as 6 and 10 wk p.i. with *H. pylori*. Biopsy specimens were obtained from study participants who had developed a persistent *H. pylori* infection (Persistent, *n* = 17, gray) and participants who had eradicated *H. pylori* (Eradicated, *n* = 7, black). Positive cells were counted per hpf, and values are shown as the mean of cells per hpf. Values are depicted as median plus interquartile ranges (Mann–Whitney *U* test followed by Bonferroni correction). The *p* values <0.017 were considered significant.

FIGURE 6. iNOS-expressing B lineage cells produce pro- and anti-inflammatory cytokines. **(A)** Detection of intracellular iNOS (left) or IFN- γ (right) within CD38⁻, CD38⁺, and CD38⁺⁺ B-LCL cells by flow cytometry. **(B)** Detection of IFN- γ within iNOS⁺ CD38⁺⁺ and iNOS⁻ CD38⁺⁺ B-LCL cells. **(C)** Relative mRNA expression of *IFN- γ* , *TNF- α* , and *IL-10* in peripheral or mucosal mBCs during *H. pylori* infection. mBCs (CD19⁺CD20⁺CD27⁺CD38⁻CD3⁻CD14⁻DAPI⁻) were isolated from PBMCs or LPLs, respectively, by FACS. The qPCR data were analyzed by the comparative C_t method ($2^{-\Delta\Delta C_t}$). All values are normalized to the expression of the housekeeping gene *GAPDH*, and the reference gene was *IL-6*. **(D)** Detection of intracellular TNF- α and IFN- γ within mucosal iNOS⁻ and iNOS⁺ mBCs (CD19⁺CD20⁺CD27⁺CD38⁻CD3⁻CD14⁻) or **(E)** PCs (CD19⁺CD20⁻CD27⁺⁺CD38⁺⁺CD3⁻CD14⁻) of an *H. pylori*-infected patient by flow cytometry. Percentages are indicated.



of *IFN- γ* , *TNF- α* , and *IL-10* mRNA than did peripheral mBCs (Fig. 6C). In PCs, the cytokine gene expression of *IFN- γ* , *TNF- α* , and *IL-10* was not detectable by qPCR. Furthermore, characterization of isolated LPLs of an *H. pylori*-infected patient by flow cytometry revealed iNOS expression by a modest proportion (2.8%) of the mucosal mBCs (CD19⁺CD20⁺CD27⁺CD38⁻) (Supplemental Fig. 2B). Intracellular cytokine staining of mucosal PCs and mBCs demonstrated coexpression of IFN- γ and TNF- α in iNOS-expressing

mBCs (33.1%, Fig. 6D), but not in iNOS⁻ mBCs, and a slightly elevated expression of TNF- α in the mucosal iNOS-expressing PCs compared with the iNOS⁻ counterparts (15.1%, Fig. 6E).

Discussion

In the current study, we identified MUM1⁺ PCs as one major cell population expressing enzymatically active iNOS in the antral mucosa of *H. pylori*-infected patients. In fact, iNOS⁺MUM1⁺ PCs

constituted approximately one third of all mucosal iNOS⁺ cells. In contrast, LPLs of control patients contained no or almost no CD19⁺ B cells or PCs, which is in agreement with previous studies (22, 33). Expression of this enzyme is not a general feature of human PCs at gastrointestinal sites because mucosal iNOS⁺ PCs were not detectable in duodenal biopsy specimens of *T. whipplei*-, HIV-, or *G. duodenalis*-infected patients, and we also detected iNOS-negative mucosal PCs in *H. pylori*-infected patients. Likewise, the analysis of transcriptome data from purified circulating PCs of patients with systemic lupus erythematosus, an autoimmune disease marked by a distinct type 1 IFN response, revealed no evidence of iNOS gene expression (J.R. Gruen and T. Doerner, unpublished data). Thus, to our knowledge, this is the first report of iNOS expression in normal, human B lineage cells, that is, IgA⁺ PCs.

To date, iNOS expression in human B lineage cells has been reported only in gastric MALT lymphoma cells (8), in B cell chronic lymphocytic leukemia cells (34), or constitutively and at low levels in EBV-transformed human B lymphocytes (26); the inducing factors, however, remain unknown. In the human lung epithelial cell line A549, functional AP-1 and NF- κ B binding elements in the promoter region were shown to confer TNF- α , IL-1, and IFN- γ cytokine inducibility (35). In this article, we demonstrate that iNOS expression in B-LCL cells that express PC marker proteins is linked to prominent production of IFN- γ . Thus, cytokines may regulate iNOS expression in B lineage cells in an autocrine/paracrine fashion. Indeed, preliminary findings from sorted memory marker-positive B cells and PCs isolated from the gastric mucosa of an *H. pylori*-infected patient are in agreement with this idea because only iNOS⁺ cells also showed detectable IFN- γ , TNF- α , or only TNF- α signals in cytofluorimetric analyses, respectively. Although speculative, a combined local presence of IFN- γ and TNF- α may constitute the signals induced by *H. pylori* that entertain iNOS expression in PCs in this infection.

Apart from the question of what exactly induces iNOS in the B lineage cells described in this article, the question arises of what its role may be. Expression of iNOS has been shown to inhibit apoptosis under certain circumstances (26, 34, 36) and could be important in PCs for their survival, as shown recently for murine, long-lived PCs residing in the bone marrow (10). In murine cells, iNOS appears to be required for the responsiveness of PCs to IL-6 and is itself induced by IL-6 (10). For human PCs, IL-6 and TNF- α are survival factors (37) and are present in *H. pylori*-infected gastric mucosa (38).

The iNOS⁺, IgA⁺ PC subset within the intestinal lamina propria has originally been described in mice upon microbial costimulation (11). In mice, deletion of TNF- α and iNOS in B lineage cells resulted in reduced IgA production. In addition, iNOS or NO has been shown to regulate IgA class switch recombination in B cells at the level of activation-induced cytidine deaminase gene expression, a key enzyme for Ig class switch (39, 40). In mice, loss of iNOS⁺ IgA⁺ PCs also resulted in altered diversification of the gut microbiota and in poor clearance of a gut-tropic pathogen, *Citrobacter rodentium* (11), indicating that this PC phenotype is linked to gut immunity. The nature of protective immunity to *H. pylori* infection remains elusive. In the present analysis, numbers of gastric iNOS⁺, IgA⁺ PCs differed significantly between groups of human volunteers who were partaking in a vaccination cum challenge study. These cells were more abundant in volunteers who were clearing the challenge infection than in individuals who remained infected. Epidemiological studies have not revealed a correlation between IgA deficiency and *H. pylori* infection status, and therefore, IgA is not considered to play a major role in *H. pylori* immunity (33, 41, 42). However, these studies could not have possibly

been designed to address a role for any iNOS⁺, IgA⁺ PCs because these were not yet known. In fact, IgA production on its own should not reveal a role in this context. We detected similar total numbers of antral mucosal IgA⁺ PCs in clearing and nonclearing vaccine study participants.

Different effector function modules of B lineage cells are known. Besides Ig, these include cytokines and, as suggested by our data, may also contain an iNOS-dependent module. Arguably, the latter would have to consider the diverse roles of the iNOS product, NO and its derivatives. In the context of *H. pylori* infection, this may include antimicrobial (4) and, potentially, tumorigenic (7, 43–47) effects during infection. Interestingly, iNOS polymorphisms have allegedly been implicated in disease outcome with respect to gastric cancer (48, 49).

Defining the inducing signals and specific role or roles of iNOS⁺ human PCs will require many more studies. However, the present report provides an incentive for these because the newly described PC phenotype constitutes a prominent leukocyte type in the antral mucosa of *H. pylori*-infected patients, and their density was increased in individuals who eradicated an experimental infection; they were not, however, a general phenotype of cells found in gastrointestinal infections.

Acknowledgments

The authors are grateful to the patients and healthy subjects for participation in this project. We thank Diana Bösel and Nadine Gehrmann for excellent technical assistance, Ulrike Erben for support of qPCR analysis, and Sarah Müller for generating the B-LCL line. We acknowledge the assistance of the Berlin-Brandenburg Center for Regenerative Therapies Flow Cytometry Laboratory.

Disclosures

The authors have no financial conflicts of interest.

References

- Wilson, K. T., and J. E. Crabtree. 2007. Immunology of *Helicobacter pylori*: insights into the failure of the immune response and perspectives on vaccine studies. *Gastroenterology* 133: 288–308.
- Mannick, E. E., L. E. Bravo, G. Zarama, J. L. Realpe, X. J. Zhang, B. Ruiz, E. T. Fontham, R. Mera, M. J. Miller, and P. Correa. 1996. Inducible nitric oxide synthase, nitrotyrosine, and apoptosis in *Helicobacter pylori* gastritis: effect of antibiotics and antioxidants. *Cancer Res.* 56: 3238–3243.
- Fu, S., K. S. Ramanujam, A. Wong, G. T. Fantry, C. B. Drachenberg, S. P. James, S. J. Meltzer, and K. T. Wilson. 1999. Increased expression and cellular localization of inducible nitric oxide synthase and cyclooxygenase 2 in *Helicobacter pylori* gastritis. *Gastroenterology* 116: 1319–1329.
- Förstermann, U., and W. C. Sessa. 2012. Nitric oxide synthases: regulation and function. *Eur. Heart J.* 33: 829–837, 837a–837d. doi:10.1093/eurheartj/ehr304.
- Murad, F. 1999. Discovery of some of the biological effects of nitric oxide and its role in cell signaling. *Biosci. Rep.* 19: 133–154.
- Ignarro, L. J. 1990. Nitric oxide. A novel signal transduction mechanism for transcellular communication. *Hypertension* 16: 477–483.
- Choudhari, S. K., M. Chaudhary, S. Bagde, A. R. Gadbaile, and V. Joshi. 2013. Nitric oxide and cancer: a review. *World J. Surg. Oncol.* 11: 118.
- Li, H. L., B. Z. Sun, and F. C. Ma. 2004. Expression of COX-2, iNOS, p53 and Ki-67 in gastric mucosa-associated lymphoid tissue lymphoma. *World J. Gastroenterol.* 10: 1862–1866.
- Pautz, A., J. Art, S. Hahn, S. Nowag, C. Voss, and H. Kleinert. 2010. Regulation of the expression of inducible nitric oxide synthase. *Nitric Oxide* 23: 75–93.
- Saini, A. S., G. N. Shenoy, S. Rath, V. Bal, and A. George. 2014. Inducible nitric oxide synthase is a major intermediate in signaling pathways for the survival of plasma cells. *Nat. Immunol.* 15: 275–282.
- Fritzi, J. H., O. L. Rojas, N. Simard, D. D. McCarthy, S. Hapfelmeier, S. Rubino, S. J. Robertson, M. Larijani, J. Gosselin, I. I. Ivanov, et al. 2011. Acquisition of a multifunctional IgA+ plasma cell phenotype in the gut. *Nature* 481: 199–203.
- Aebischer, T., D. Bumann, H. J. Epple, W. Metzger, T. Schneider, G. Cherepnev, A. K. Walduck, D. Kunkel, V. Moos, C. Lodenkemper, et al. 2008. Correlation of T cell response and bacterial clearance in human volunteers challenged with *Helicobacter pylori* revealed by randomised controlled vaccination with Ty21a-based *Salmonella* vaccines. *Gut* 57: 1065–1072.
- Graham, D. Y., A. R. Opekun, M. S. Osato, H. M. El-Zimaity, C. K. Lee, Y. Yamaoka, W. A. Qureshi, M. Cadoz, and T. P. Monath. 2004. Challenge model for *Helicobacter pylori* infection in human volunteers. *Gut* 53: 1235–1243.

14. Loddenkemper, C., I. Anagnostopoulos, M. Hummel, K. Jöhrens-Leder, H. D. Foss, F. Jundt, T. Wirth, B. Dörken, and H. Stein. 2004. Differential Emu enhancer activity and expression of BOB.1/OBF.1, Oct2, PU.1, and immunoglobulin in reactive B-cell populations, B-cell non-Hodgkin lymphomas, and Hodgkin lymphomas. *J. Pathol.* 202: 60–69.
15. Falini, B., M. Fizzotti, A. Pucciarini, B. Bigerna, T. Marafioti, M. Gambacorta, R. Pacini, C. Alunni, L. Natali-Tanci, B. Ugolini, et al. 2000. A monoclonal antibody (MUM1p) detects expression of the MUM1/IRF4 protein in a subset of germinal center B cells, plasma cells, and activated T cells. *Blood* 95: 2084–2092.
16. Shacklett, B. L., O. Yang, M. A. Hausner, J. Elliott, L. Hultin, C. Price, M. Fuerst, J. Matud, P. Hultin, C. Cox, et al. 2003. Optimization of methods to assess human mucosal T-cell responses to HIV infection. *J. Immunol. Methods* 279: 17–31.
17. Pelloquin, F., J. P. Lamelin, and G. M. Lenoir. 1986. Human B lymphocytes immortalization by Epstein-Barr virus in the presence of cyclosporin A. *In Vitro Cell. Dev. Biol.* 22: 689–694.
18. Mei, H. E., T. Yoshida, W. Sime, F. Hiepe, K. Thiele, R. A. Manz, A. Radbruch, and T. Dörner. 2009. Blood-borne human plasma cells in steady state are derived from mucosal immune responses. *Blood* 113: 2461–2469.
19. Cortese-Krott, M. M., A. Rodriguez-Mateos, G. G. Kuhnle, G. Brown, M. Feelsch, and M. Kelm. 2012. A multilevel analytical approach for detection and visualization of intracellular NO production and nitrosation events using diaminofluoresceins. *Free Radic. Biol. Med.* 53: 2146–2158.
20. Nagano, T. 1999. Practical methods for detection of nitric oxide. *Luminescence* 14: 283–290.
21. Adams, B., P. Dörfler, A. Aguzzi, Z. Kozmik, P. Urbánek, I. Maurer-Fogy, and M. Busslinger. 1992. Pax-5 encodes the transcription factor BSAP and is expressed in B lymphocytes, the developing CNS, and adult testis. *Genes Dev.* 6: 1589–1607.
22. Bhuiyan, T. R., F. Qadri, P. K. Bardhan, M. M. Ahmad, B. Kindlund, A. M. Svennerholm, and A. Lundgren. 2008. Comparison of mucosal B- and T-cell responses in *Helicobacter pylori*-infected subjects in a developing and a developed country. *FEMS Immunol. Med. Microbiol.* 54: 70–79.
23. Carter, K. L., E. Cahir-McFarland, and E. Kieff. 2002. Epstein-Barr virus-induced changes in B-lymphocyte gene expression. *J. Virol.* 76: 10427–10436.
24. Wroblewski, J. M., A. Copple, L. P. Batson, C. D. Landers, and J. R. Yannelli. 2002. Cell surface phenotyping and cytokine production of Epstein-Barr virus (EBV)-transformed lymphoblastoid cell lines (LCLs). *J. Immunol. Methods* 264: 19–28.
25. Hur, D. Y., M. H. Lee, J. W. Kim, J. H. Kim, Y. K. Shin, J. K. Rho, K. B. Kwack, W. J. Lee, and B. G. Han. 2005. CD19 signalling improves the Epstein-Barr virus-induced immortalization of human B cell. *Cell Prolif.* 38: 35–45.
26. Mannick, J. B., K. Asano, K. Izumi, E. Kieff, and J. S. Stamler. 1994. Nitric oxide produced by human B lymphocytes inhibits apoptosis and Epstein-Barr virus reactivation. *Cell* 79: 1137–1146.
27. Pistoia, V., F. Cozzolino, A. Rubartelli, M. Torcia, S. Roncella, and M. Ferrarini. 1986. In vitro production of interleukin 1 by normal and malignant human B lymphocytes. *J. Immunol.* 136: 1688–1692.
28. Rochford, R., M. J. Cannon, R. E. Sabbe, K. Adusumilli, G. Picchio, J. M. Glynn, D. J. Noonan, D. E. Mosier, and M. V. Hobbs. 1997. Common and idiosyncratic patterns of cytokine gene expression by Epstein-Barr virus transformed human B cell lines. *Viral Immunol.* 10: 183–195.
29. Hutchins, D., B. B. Cohen, and C. M. Steel. 1990. Production and regulation of interleukin 6 in human B lymphoid cells. *Eur. J. Immunol.* 20: 961–968.
30. Sung, S. S., L. K. Jung, J. A. Walters, W. Chen, C. Y. Wang, and S. M. Fu. 1988. Production of tumor necrosis factor/cachectin by human B cell lines and tonsillar B cells. *J. Exp. Med.* 168: 1539–1551.
31. Burdin, N., C. Péronne, J. Banchereau, and F. Rousset. 1993. Epstein-Barr virus transformation induces B lymphocytes to produce human interleukin 10. *J. Exp. Med.* 177: 295–304.
32. Miyauchi, K., E. Urano, H. Yoshiyama, and J. Komano. 2011. Cytokine signatures of transformed B cells with distinct Epstein-Barr virus latencies as a potential diagnostic tool for B cell lymphoma. *Cancer Sci.* 102: 1236–1241.
33. Mattsson, A., M. Quiding-Järbrink, H. Lönröth, A. Hamlet, I. Ahlstedt, and A. Svennerholm. 1998. Antibody-secreting cells in the stomachs of symptomatic and asymptomatic *Helicobacter pylori*-infected subjects. *Infect. Immun.* 66: 2705–2712.
34. Hammadi, A., C. Billard, A. M. Faussat, and J. P. Kolb. 2008. Stimulation of iNOS expression and apoptosis resistance in B-cell chronic lymphocytic leukemia (B-CLL) cells through engagement of Toll-like receptor 7 (TLR-7) and NF-kappaB activation. *Nitric Oxide* 19: 138–145.
35. Chu, S. C., J. Marks-Konczalik, H. P. Wu, T. C. Banks, and J. Moss. 1998. Analysis of the cytokine-stimulated human inducible nitric oxide synthase (iNOS) gene: characterization of differences between human and mouse iNOS promoters. *Biochem. Biophys. Res. Commun.* 248: 871–878.
36. Forrester, K., S. Ambs, S. E. Lupold, R. B. Kapust, E. A. Spillare, W. C. Weinberg, E. Felley-Bosco, X. W. Wang, D. A. Geller, E. Tzeng, et al. 1996. Nitric oxide-induced p53 accumulation and regulation of inducible nitric oxide synthase expression by wild-type p53. *Proc. Natl. Acad. Sci. U S A* 93: 2442–2447.
37. Cassese, G., S. Arce, A. E. Hauser, K. Lehnert, B. Moewes, M. Mostarac, G. Muehlinghaus, M. Szyska, A. Radbruch, and R. A. Manz. 2003. Plasma cell survival is mediated by synergistic effects of cytokines and adhesion-dependent signals. *J. Immunol.* 171: 1684–1690.
38. Crabtree, J. E., T. M. Shallcross, R. V. Heatley, and J. I. Wyatt. 1991. Mucosal tumour necrosis factor alpha and interleukin-6 in patients with *Helicobacter pylori* associated gastritis. *Gut* 32: 1473–1477.
39. Lee, M. R., G. Y. Seo, Y. M. Kim, and P. H. Kim. 2011. iNOS potentiates mouse Ig isotype switching through AID expression. *Biochem. Biophys. Res. Commun.* 410: 602–607.
40. Tezuka, H., Y. Abe, M. Iwata, H. Takeuchi, H. Ishikawa, M. Matsushita, T. Shiohara, S. Akira, and T. Ohteki. 2007. Regulation of IgA production by naturally occurring TNF/iNOS-producing dendritic cells. *Nature* 448: 929–933.
41. Akhiani, A. A., A. Stensson, K. Schön, and N. Y. Lycke. 2005. IgA antibodies impair resistance against *Helicobacter pylori* infection: studies on immune evasion in IL-10-deficient mice. *J. Immunol.* 174: 8144–8153.
42. Bogstedt, A. K., S. Nava, T. Wadström, and L. Hammarström. 1996. *Helicobacter pylori* infections in IgA deficiency: lack of role for the secretory immune system. *Clin. Exp. Immunol.* 105: 202–204.
43. Naito, Y., T. Takagi, H. Okada, Y. Nukigi, K. Uchiyama, M. Kuroda, O. Handa, S. Kokura, N. Yagi, Y. Kato, et al. 2008. Expression of inducible nitric oxide synthase and nitric oxide-modified proteins in *Helicobacter pylori*-associated atrophic gastric mucosa. *J. Gastroenterol. Hepatol.* 23(Suppl. 2): S250–S257.
44. Sheh, A., C. W. Lee, K. Masumura, B. H. Rickman, T. Nohmi, G. N. Wogan, J. G. Fox, and D. B. Schauer. 2010. Mutagenic potency of *Helicobacter pylori* in the gastric mucosa of mice is determined by sex and duration of infection. *Proc. Natl. Acad. Sci. U S A* 107: 15217–15222.
45. Cianchi, F., C. Cortesini, O. Fantappiè, L. Messerini, N. Schiavone, A. Vannacci, S. Nistri, I. Sardi, G. Baroni, C. Marzocca, et al. 2003. Inducible nitric oxide synthase expression in human colorectal cancer: correlation with tumor angiogenesis. *Am. J. Pathol.* 162: 793–801.
46. Chen, C. N., F. J. Hsieh, Y. M. Cheng, K. J. Chang, and P. H. Lee. 2006. Expression of inducible nitric oxide synthase and cyclooxygenase-2 in angiogenesis and clinical outcome of human gastric cancer. *J. Surg. Oncol.* 94: 226–233.
47. Song, Z. J., P. Gong, and Y. E. Wu. 2002. Relationship between the expression of iNOS, VEGF, tumor angiogenesis and gastric cancer. *World J. Gastroenterol.* 8: 591–595.
48. Rafiei, A., V. Hosseini, G. Janbabai, B. Fazli, A. Ajami, Z. Hosseini-Khah, J. Gilbreath, and D. S. Merrell. 2012. Inducible nitric oxide synthetase genotype and *Helicobacter pylori* infection affect gastric cancer risk. *World J. Gastroenterol.* 18: 4917–4924.
49. Goto, Y., T. Ando, M. Naito, H. Goto, and N. Hamajima. 2006. Inducible nitric oxide synthase polymorphism is associated with the increased risk of differentiated gastric cancer in a Japanese population. *World J. Gastroenterol.* 12: 6361–6365.